

Image inpainting in remote sensing

Santiago Passos[‡] and Alejandro Rojas[‡]
spassos@eafit.edu.co, arojasb3@eafit.edu.co

[†]Mathematical Engineering, Universidad EAFIT

November 13, 2019

1 Information

1.1 Satellite Images

This are images taken from satellites, their overall composition consists in different bands (R,G,B, Near-Infrared, etc). However the bands vary depending on the device the image was taken. For example, the bands for the Landsat 8 satellite images can be seen on Table 1. We will show a small description on each of the Landsat 8 bands made by Charlie Loyd (2013):

Band 1: Senses deep blues and violets. Blue light is hard to collect from space because it's scattered easily by tiny bits of dust and water in the air, and even by air molecules themselves. Its 2 main uses are: imaging shallow water, and tracking fine particles of dust and smoke.

Band 2, 3 and 4: Visible blue, green and red. This band covers the visible spectrum of Humans.

Band 4: NIR band. It is important because chrolophyll in healthy plants reflect it, helping to calculate indexes like the Normalized difference vegetation index (NDVI), which can be seen on Image 1, where areas with higher values show vegetation on the city.

Band 6 and 7: Shortwave infrared (SWIR). They are important for telling wet earth from dry earth and can help see differences in rocks and soils that looked similar in other bands.

Band 8: Panchromatic band. Combines all colors in one channel, increasing its sharpness but loosing the different colors.

Band 9: Useful for capturing cirrus clouds.

Inpainting techniques patchmatch Statistical methods Machine Learning

1.2 Inpainting

The problem of filling missing parts of images has been existing for a long time and It has many applications like image restoration, special effects, image coding and more. The practice of inpainting is filling those parts of the images with either available information of the picture or from previously known information learned in a extensive training. One of the most importants objectives of inpainting is that the filled part won't be identified by a casual observer, which makes it a time consuming and overall difficult process Janarthanan & Jananii (2012).

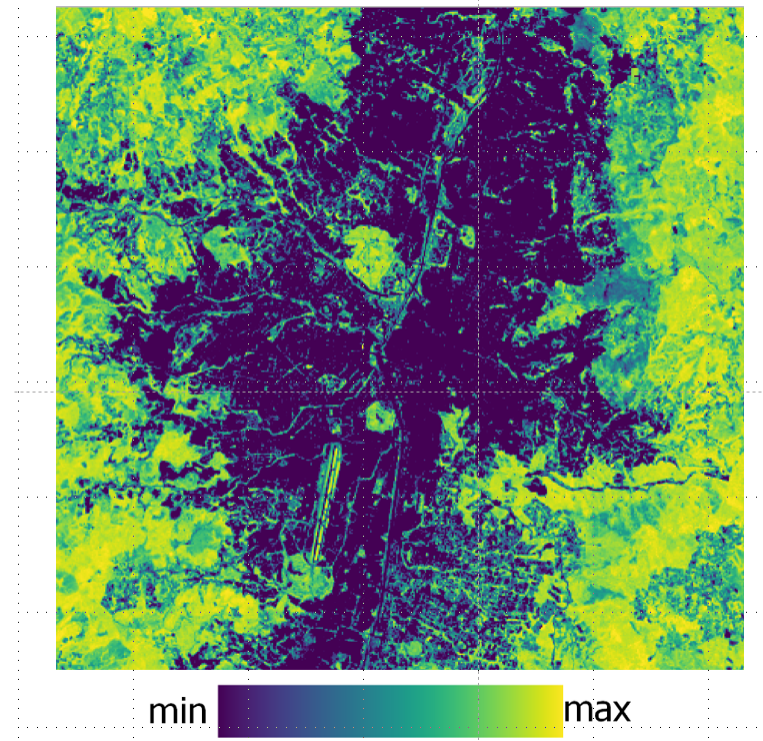


Figure 1: NDVI for Medellín from a Landsat 8 image from December 2017.

We studied 3 different methods for inpainting, two using differential equations and another one using deep convolutional neural networks:

1.3 Differential Equations algorithms

The approaches of Telea (2004) and Bertalmio *et al.* (2001) are based on partial differential equations, where the images are treated as fluid or waves, and the objective is to solve the equation set by the mask. On this document we will refer as Telea and Navier - Stokes respectively.

1.4 Partial Convolutional Layers

They propose the use of partial convolutions, where the convolution is conditioned on only valid pixels. They generated a mechanism to automatically generate an updated mask for the next layer as part of the forward pass. This model outperforms Our model outperforms other methods for irregular masks (Liu *et al.* , 2018).

They propose the use of partial convolutions with an automatic mask update step for achieving state-of-the-art on image inpainting and demonstrate that substituting convolutional layers with partial convolutions and mask updates in a U-Net can achieve state-of-the-art inpainting results (Liu *et al.* , 2018).

The following equation is used in each partial convolutional layer. Where W are the filters weights for the convolution filter and b is the corresponding bias. X are the features values for the

Table 1: Landsat 8 Bands.

Band	Name	Wavelength	Pixel Size
1	Visible	0.43 - 0.45 μ m	30 m
2	Visible	0.45 - 0.51 μ m	30 m
3	Visible	0.53 - 0.59 μ m	30 m
4	Red	0.64 - 0.67 μ m	30 m
5	Near - Infrared	0.85 - 0.88 μ m	30 m
6	SWIR 1	1.57 - 1.65 μ m	30 m
7	SWIR 2	2.11 - 2.29 μ m	30 m
8	PAN	0.50 - 0.68 μ m	30 m
9	Cirrus	1.36 - 1.38 μ m	30 m

current image and M is the corresponding binary mask.

$$\begin{cases} \mathbf{W}^T(\mathbf{X} \odot \mathbf{M}) \frac{\text{sum}(1)}{\text{sum}(\mathbf{M})} + b, & \text{if } \text{sum}(\mathbf{M}) > 0 \\ 0, & \text{otherwise} \end{cases}$$

2 Problem definition

The presence of clouds is a common issue in satellite images processing, finding good images to work with basically depends on the amount of clouds preset. Here is where inpainting appears as a solution, filling the missing information and enabling the analysis of the image. This can be seen on Image 2.

However the inpainting algorithm used must be powerful enough to separate between different land covers and keep the geometry of the urban areas. This is one of the principal challenges of this problem.

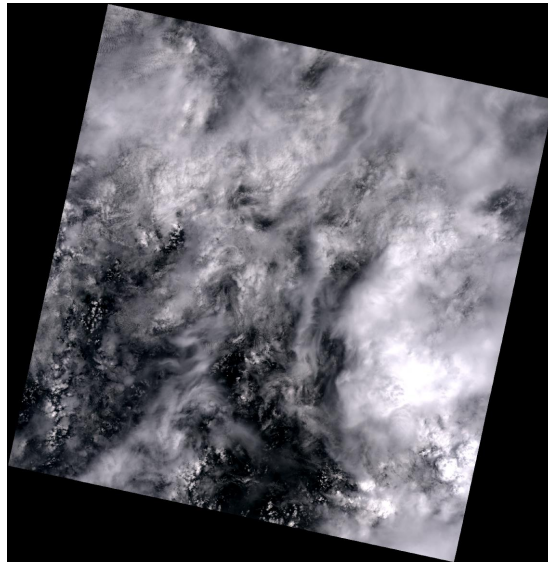


Figure 2: Antioquia Landsat 8 image from October 2016.

3 Objective

Test the effectiveness of the methods proposed by Yu *et al.* (2018) and Liu *et al.* (2018) in faces, places and satellite images.

4 Results

We tested the three algorithms with five different images, 2 of them were portions of a Sentinel image of Medellín from December 2017. The results can be seen on Image 3. The first Image was taken from the Celeba database, the second and third images from ImageNet database and the forth and fifth are portions of a Medellín picture from December 2017 of Sentinel Satelite.

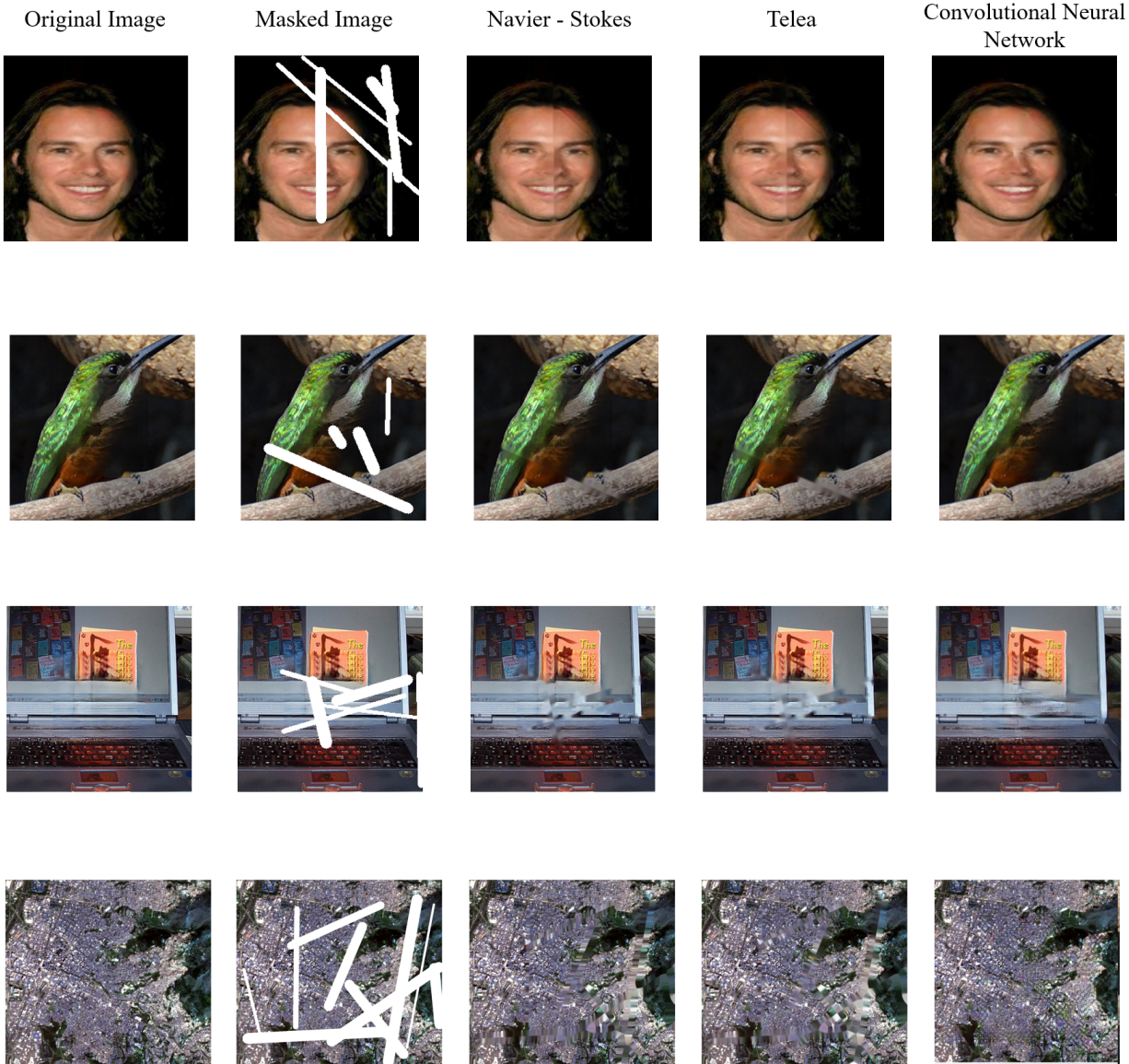




Figure 3: Results for the different images and algorithms.

It can be seen how the model based on machine learning showed the best results overall in quality, for the celeba and imagenet images. For the satellite images despite apparently showing a good result on Image 3, the real construction was a lot different from the original image which would make data analysis from that image erroneous or biased. The difference can be seen on Image 4.



Figure 4: Zoom of a portion of the Urban Area inpainting.



Figure 5: Zoom of a portion of Rural Area inpainting.

5 Conclusions

All algorithms work for common images, however they didn't show good results with satellite imagery. A lot of information was lost with the ones based on partial differential equations, while the information was distorted on the machine learning approach, making harder any analysis of the inpainted images.

For future work it is recommended to train the machine learning model with satellite imagery datasets and check its performance.

References

- Bertalmio, M., Bertozzi, A. L., & Sapiro, G. 2001. Navier-stokes, fluid dynamics, and image and video inpainting. **1**(Dec), I–I.
- Charlie Loyd. 2013. Putting Landsat 8's Bands to Work.
- Janarthanan, V., & Jananii, G. 2012. A Detailed Survey on Various Image Inpainting Techniques. *Bonfring International Journal of Advances in Image Processing*, **2**(2), 01–03.
- Liu, Guilin, Reda, Fitsum, Shih, Kevin, Wang, Ting-Chun, Tao, Andrew, & Catanzaro, Bryan. 2018. Image Inpainting for Irregular Holes Using Partial Convolutions. 04.
- Telea, Alexandru. 2004. An Image Inpainting Technique Based on the Fast Marching Method. *Journal of Graphics Tools*, **9**(01).
- Yu, Jiahui, Lin, Zhe, Yang, Jimei, Shen, Xiaohui, Lu, Xin, & Huang, Thomas S. 2018. Generative Image Inpainting with Contextual Attention. *arXiv preprint arXiv:1801.07892*.